Physicochemical, Antibacterial, and Cytotoxic Properties of Composite Materials Based on Biodegradable Poly (Lactic-Co-Glycolic Acid) Functionalized with Zno Nanoparticles

Dmitriy Burmistrov[1,*], *Dmitriy* Serov[1], *Daria* Grigorieva[2] and *Alexander* Simakin[1]

[1]Prokhorov General Physics Institute of the Russian Academy of Sciences, Moscow, Russia
[2]Belarusian State University, Minsk, Belarus

Abstract. One of the tasks of modern nanotechnology is the creation of new materials with a wide range of applications and good antibacterial activity. In this work, we developed a new composite material based on poly(lactic-co-glycolic acid) and zinc oxide nanoparticles. The resulting material had a smooth surface without microdefects. The polymer matrix did not affect the generation of reactive oxygen species, 8-oxoguanine, and long-lived protein forms. The addition of ZnO-NPs enhanced the generation of these compounds. The addition of ZnO-NPs to the polymer at a concentration of 0.001-0.1 wt% made it possible to achieve a significant bacteriostatic effect, while not affecting the growth, division, and viability of eukaryotic cells. The resulting composite material is of great interest for biomedical use and the food industry due to controlled biodegradability and antibacterial activity.

1 Introduction

Nanotechnologies are currently being used in various areas of human life, including biomedicine, the food industry, and agriculture [1–3]. Of particular interest is the use of nanoparticles (NPs) of metals and metal oxides as antibacterial agents [4]. Numerous studies have demonstrated the activity of nanosized zinc oxide against both Gram-positive and Gram-negative bacteria [5-7]. One of the main advantages of ZnO-NPs over other nanomaterials is their high antibacterial efficacy at low concentrations (0.16–5.00 mM), activity against a wide range of bacterial strains, relatively low cost, and ease of synthesis [8]. ZnO-NPs realize antibacterial properties due to the generation of reactive oxygen species (ROS) in the course of photocatalytic reactions. The resulting ROS, hydroxyl radicals (OH•), superoxide anions (O_2^-), and hydrogen peroxide (H_2O_2) cause oxidative stress and damage cell biopolymers [9, 10]. One of the promising strategies for increasing the antibacterial properties and controlling the biocompatibility of NPs is the creation of polymer-NP composites. The following are used as matrices for creating composites: chitosan, gelatin, polyvinyl alcohol (PVA), polylactate (PLA), polypropylene,

* Corresponding author: dmitriiburmistroff@gmail.com

polyurethane, borosiloxane, poly(glycolide-co-lactide) (PLGA), etc. [11-13]. PLGA is a polymer with good biocompatibility and biodegradability [14]. In the body, PLGA is degraded to polyglycolic acid (PGA) and polylactic acid (PLA). Successful creation of composites based on PLGA containing NPs of metals and metal oxides was noted [15–18]. The main advantage of PLGA is its ability to adjust biodegradability in the recipient's body by changing the ratio of lactide/glycolide monomers in the composition [19].

In this study, we synthesized a PLGA/ZnO-NPs composite material using low-temperature technology. The physicochemical properties of the obtained samples of materials were characterized using methods such as dynamic light scattering, electrophoretic light scattering, absorption spectroscopy, transmission electron microscopy, modulation-interference microscopy. We also studied *in vitro* antibacterial and cytotoxic properties of newly synthesized composites with different concentrations of ZnO-NPs in the composition (0.1; 0.01; 0.001 wt%) against *E. coli* and SH-SY5Y cell line.

2 Materials and methods

2.1. Synthesis and characterization of ZnO-NPs

Thelaser ablation in a liquid method (deionized water) was used for the synthesis of ZnO-NPs. A pulsed ytterbium-doped fiber laser was used. Laser radiation parameters: λ=1064 nm, τ=4–200 ns; ν=20 kHz; average power up to 20 W; E=1 mJ. The liquid layer above the target (metal zinc plate) was about 1 mm. Irradiation time varied in the range of 5-20 minutes. The hydrodynamic diameter and zeta potential of the resulting NPs were determined using a Zetasizer Ultra Red Label (Malvern Panalytical, UK). The NPs diameter was confirmed using a CPS 24000 [20]. Morphological features (shape, topology), as well as the elemental composition of NPs, were studied using a Libra 200 FE HR transmission electron microscope (Carl Zeiss, Germany) in combination with a JED-2300 energy-dispersive X-ray spectrometer. The colloid composition of the obtained NPs was confirmed using Cintra 4040 (GBC Scientific Equipment, Australia).

2.2. Preparation and characterization of the composite material

To obtain a PLGA/ZnO-NPs composite material, a technology developed earlier was used. Briefly, the composite material was prepared by preliminary preparation of a 3% solution of PLGA (Creative Biolabs, USA) in chloroform with stirring until a homogeneous state for 1 h at a solution temperature of 57°C. Next, a colloidal solution of zinc oxide NPs of the required concentration was added to the dissolved PLGA [21]. The material was heated to 40°C and then rolled through rollers. As a result, a composite film with a thickness of about 1000 μm was obtained, from which rectangular samples were cut. The troubleshooting of the material surface was carried out using atomic force microscopy, and the distribution of NPs in the material was evaluated using modulation interference microscopy.

2.3. Quantification of ROS

The concentration of hydrogen peroxide formed in aqueous solutions was estimated from the intensity of chemiluminescence of the luminol-p-iodophenol-horseradish peroxidase system. Chemiluminescence was measured on a highly sensitive Biotox-7A chemiluminometer (Engineering Center - Ecology, Russia). Samples of the films of the material were placed in polypropylene vials (Beckman, USA) with the addition of 1 mL of the "counting solution" prepared immediately before the measurement, containing 1 mM

Tris-HCl buffer pH 8.5, 50 μM p-iodophenol, 50 μM luminol, 10 nM horseradish peroxidase. The sensitivity of this method is <1 nM [22]. To quantify the content of hydroxyl radicals in aqueous solutions, the reaction with coumarin-3-carboxylic acid (CCA) was used. The hydroxylation reaction produces the fluorescent product 7-hydroxycoumarin-3-carboxylic acid (7-OH-CCA). Fluorescence of 7-OH-CCA) was recorded using a JASCO 8300 spectrofluorimeter (JASCO, Japan) at λex = 400 nm, λem = 450 nm.

2.4. Measurement of the concentration of the formed active long-lived forms of proteins

The number of long-lived reactive forms of proteins (LLRPF) was estimated from the intensity of chemiluminescence of protein solutions after heating after 40°C for 2 hours. All samples were stored in the dark at room temperature for 30 min after exposure. The measurements were carried out in 20 mL polypropylene vials (Beckman, USA) in the dark at room temperature on a highly sensitive Biotox-7A chemiluminometer (Engineering Center - Ecology, Russia). Protein solutions not subjected to heating were used as controls [23].

2.5. Quantitative determination of 8-oxoguanine in DNA *in vitro* by ELISA

To quantify 8-oxoguanine in DNA, a non-competitive enzyme-linked immunosorbent assay (ELISA) was used using monoclonal antibodies specific for 8-oxoguanine (anti-8-OG antibodies). The formation of an antigen-antibody complex with mouse antibodies against 8-OG (at a dilution of 1: 2000) was carried out in a blocking solution (100 μl/well) by incubation for 3 h at 37°C. A complex with a conjugate (immunoglobulin to mouse Fc fragments labeled with horseradish peroxidase (1:1000)) was formed by incubation for 1.5 h at 37°C in blocking solution (80 μl/well). A chromogenic substrate containing 18.2 mM ABTS and hydrogen peroxide (2.6 mM) in 75 mM citrate buffer, pH 4.2 (100 μl/well) was added to each well. Reactions were stopped after formation of visible color by adding an equal volume of 1.5 mM NaN_3 in 0.1 M citrate buffer (pH 4.3). The optical density of the samples was measured on a plate spectrophotometer (Titertek Multiscan, Finland) at λ = 405 nm. The method was described in more detail earlier [24].

2.6. Evaluation of the antibacterial activity of the samples

The antibacterial activity of the obtained PLGA/ZnO-NPs composites was evaluated on the gram-negative bacterium Escherichia coli. Film samples were sterilized in 70% ethanol for 30 min. A sample of the material in the form of a film was put on a sterile hoop, on which then liquid LB nutrient medium with a known number of CFU was placed. The resulting construct was placed in an ES-20 shaker-incubator (Biosan, Latvia) and cultivated at 37°C, at 150 rpm for 24 hours. Using microscopy, drop spectrometry, and the previously developed algorithm for detecting optically dense objects in a frame, the concentration of bacterial cells after cultivation was estimated.

2.7. Cytotoxicity study on SH-SY5Y cells

The human neuroblastoma cell line SH-SY5Y was used as an *in vitro* test system. These cells are widely used to study the development and differentiation of nerve cells *in vitro*. Cultivation was carried out in DMEM medium with L-glutamine (Biolot, Russia)

containing 10% fetal calf serum (Gibco, USA), 100 U/mL penicillin, and 100 μg/mL streptomycin (PanEco, Russia) in a CO_2 incubator S-Bt Smart Biotherm (Biosan, Latvia) at 37°C and 5% CO_2. Samples of PLGA/ZnO-NPs composite were placed one by one into Ø 35 mm Petri dishes. A suspension of SH-SY5Y cells (104 cells/cm2, 3 ml) was placed on the surface of the samples and cultured for 72 hours. The viability of cell cultures was assessed by staining the cultures with fluorescent dyes Hoechst 33342 and propidium iodide (PI) (Sigma, USA) at concentrations of 2 μg/ml each. To register the growth of cell cultures on the surface of samples of PLGA/ZnO-NPs composites, a Leica DMI6000 system (Leica, Germany) was used. A number of pictures were taken on a randomly selected field of the crop in question in transmitted light, with filters for Hoechst and PI. The number of non-viable cells, the cell culture density, the percentage of cell-free surface area, and the mitotic index were evaluated using the ImageJ software as the main parameters that determine the growth and development of cells.

2.8. Data processing

Data were analyzed using GraphPad Prism 8 and Origin software and presented as mean ± standard error of the mean. Data from at least three independent experiments were used for averaging. The statistical significance of differences was assessed using Student's t-test.

3 Results and discussion

ZnO-NPs were synthesized by laser ablation in water. This method makes it possible to obtain stable colloidal solutions of NPs with a narrow particle size distribution and does not require the use of stabilizing agents and reducing agents [25, 26]. The concentration and hydrodynamic NP were determined using dynamic light scattering. The colloidal solution contained ~450 million NPs/mL with an average hydrodynamic diameter of 47 nm (Fig. 1a). The size distribution of NPs was monomodal with a distribution half-width of about 45–60 nm. Also, using electrophoretic light scattering, the profile of the NP zeta potential was determined, which was distributed in the range from 6 to 40 nm with a maximum of 15 mV (Fig. 1b). Absorption spectroscopy confirmed the composition of the obtained nanoparticles corresponding to zinc oxide (Fig. 1c). Morphology analysis using TEM showed the presence in the colloidal solution of nanoparticles with a rod-like morphology, about 40-70 nm long (Fig. 1d). A number of papers reported that the antibacterial properties of nanoparticles may depend on the morphological features of the particles, which is associated with a change in the specific surface area and the number of adsorption centers on the particle surface [27]. Energy-dispersive X-ray spectrometry was used to determine the chemical composition and purity of the obtained NPs. The content of zinc and oxygen in the composition of NPs was revealed. The resulting NPs contained ~75% ZnO and ~25% zinc metal (Fig. 1e).

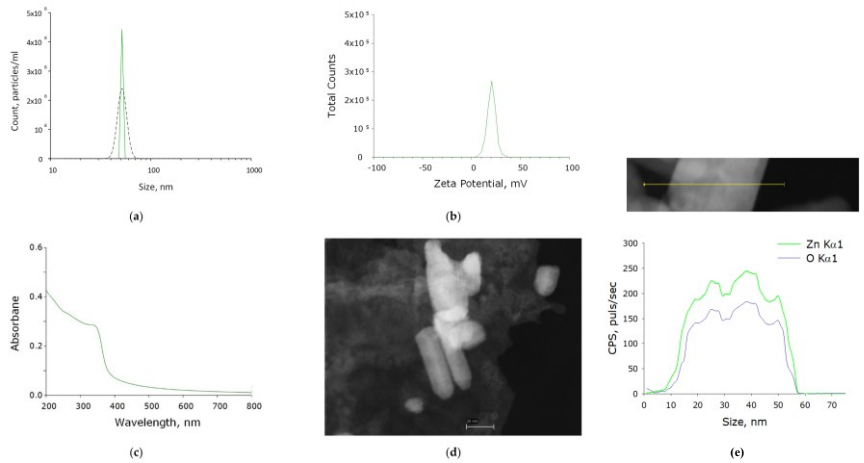

Fig. 1. Physicochemical properties of ZnO-NPs. Concentration (solid line) and size distribution (dashed black line) of zinc oxide NPs (a); distribution of the zeta potential of zinc oxide NPs (b); optical absorption spectrum of an aqueous colloidal solution of zinc oxide NPs (c); TEM image of a group of zinc oxide NPs (d), EDX profile of NPs (bottom) and enlarged measurement site (top) (e)

The PLGA/ZnO-NPs composites were fabricated using the low-temperature technology developed by us earlier. Using the atomic force microscope method, it was shown that the resulting composite material had a uniform and smooth surface without cracks, ruptures, and other artifacts (Fig. 2a).

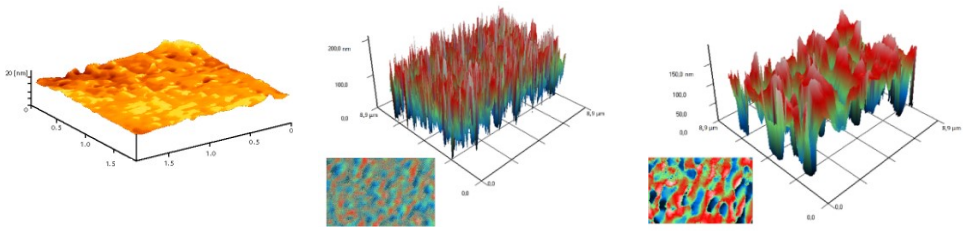

Fig. 2. Analysis of the surface of the composite material and the distribution of NPs in the polymer matrix: Reconstruction of the microrelief of the surface of the composite sample based on PLGA, performed using an atomic force microscope (a). Images of PLGA, without NPs (b) and composite material with a concentration of 0.1% NPs (c), obtained using MIM. On "b" and "c" three-dimensional visualization of the material surface profile is presented. Axes X and Y - the size of the investigated surface in microns. The Z-axis is the relief as a phase change expressed in nm. In the lower left corner of figures "b" and "c" there is a 2D image (height map of the material surface)

Using MIM, it was found that the surface of PLGA without NPs did not have a pronounced structure (Fig. 2b). The addition of ZnO-NPs led to the formation of domains that were distinguished by a change in the phase of laser radiation (Fig. 2c). It was found that ZnO-NPs are distributed in the volume of PLGA in the form of domain structures, the size of which reached several microns at the highest concentration (Fig. 2c). Thus, the distribution of ZnO-NPs in the PLGA/ZnO-NPs composite was non-uniform.

The ability of a material to exhibit antibacterial properties may be due to the structure of the surface, including due to electrostatic or mechanical damage to cells [28], and the release of biologically active compounds by the material [29]. Often, reactive oxygen species are used as such compounds. As is known, ROS are highly reactive compounds that damage macromolecules (membrane lipids, proteins, and nucleic acids) [30]. In this regard,

the ability of the resulting PLGA/ZnO-NPs composite to form ROS: hydrogen peroxide and hydroxyl radicals was studied. It was found that pure PLGA had no effect on the generation of ROS in aqueous solution. However, the PLGA/ZnO-NPs composite increased the rate of formation of hydrogen peroxide (Fig. 3a) and hydroxyl radicals (Fig. 3b) at all studied concentrations of ZnO-NPs. An increase in the concentration of ZnO-NPs in the composition of the composite contributed to an increase in the rate of ROS generation. In particular, composites with the highest concentration of ZnO-NPs (0.1%) increased the formation of H_2O_2 by ~5 times and OH radicals by ~2.5 times.

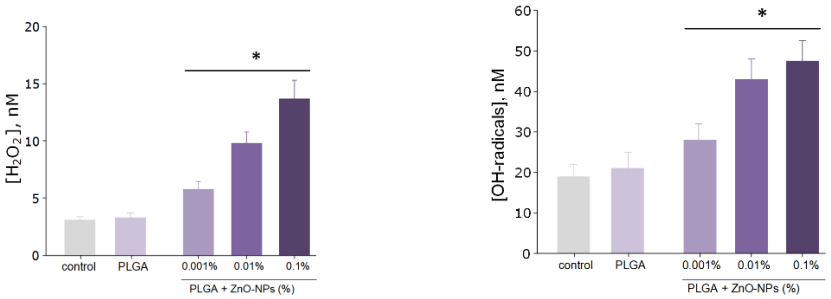

(a) (b)

Fig. 3. Effect of the PGLA/ZnO-NPs composite material on the generation of ROS: generation of hydrogen peroxide (2 h, 40°C) (a); formation of hydroxyl radicals (2 h, 80°C) (b); * - statistically significant difference with the control group ($p < 0.05$). Data are presented as mean with SEM.

Nucleic acids are often a target for ROS, especially in bacterial cells [31]. The key product of oxidative damage to DNA is 8-oxoguanine, which causes adenine mismatch [32]. The accumulation of 8-oxoguanine in DNA also plays a role in the development of cancer and in the aging process [33]. On the other hand, ROS cause oxidative damage to protein macromolecules with the formation of LLRPF that can cause cellular mutations and transformations, and are also a source of secondary free radicals that cause subsequent damage to biomolecules [23, 34]. The addition of ZnO-NPs to the composition of PLGA increased the rate of formation of 8-oxoguanine in DNA in proportion to the increase in the concentration of ZnO-NPs. At a ZnO-NP concentration of 0.001%, an increase in the rate of formation of 8-oxoguanine in DNA by 1.5 times was observed; at a concentration of ZnO-NPs of 0.01% by 2.3 times; at a concentration of 0.1% by 2.8 times (Fig. 4a). Also, we studied the effect of PLGA/ZnO-NPs composite on the formation of LLRPF. The addition of ZnO-NPs to the polymer led to a statistically significant increase in the rate of formation of LLRPF (Fig. 4b). The addition of ZnO-NPs did not affect the half-life of LLRPF, which was about 4-5 hours. The study of the effect of PLGA/ZnO-NP composites on the growth and development of *E. coli* bacterial cultures (Fig. 4c) showed that PLGA without ZnO-NPs in the composition does not affect the growth and development of bacterial cells. The addition of ZnO-NPs to PLGA led to a sharp decrease in the number of bacterial cells on the surface of the composite. An increase in the concentration of ZnO-NPs led to an increase in the bacteriostatic effect. The number of cells on the surface of the composite with 0.001% ZnO-NPs decreased by 2 times; with 0.01% ZnO-NPs by 10 times. The PLGA/ZnO-NPs composite containing 0.1% ZnO-NPs had perfect bacteriostatic properties. In general, the results of microbiological studies are in good agreement with other data demonstrating the ability of nanomaterials based on metal oxides to inhibit the growth and development of bacteria [8,35,36].

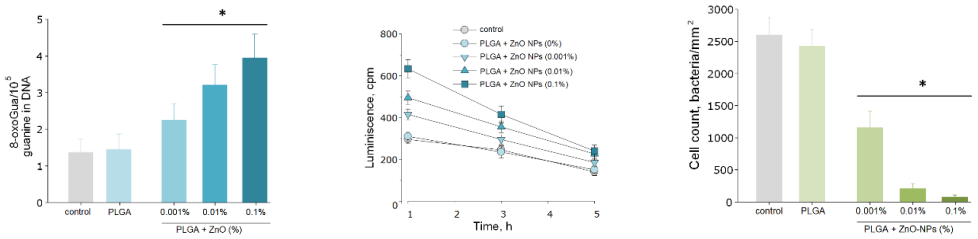

(a) (b) (c)

Fig. 4. Effect of the PGLA/ZnO-NPs material on the 8-oxoguanine in DNA formation (2h, 45°C) (a); LLRPF formation (2h, 40°C) (b); microbiological test results against *E. coli* (c).* - statistically significant difference with the control group ($p<0.05$). Data are presented as mean with SEM.

We also studied the cytotoxic effects of PLGA/ZnO-NPs on the SH-SY5Y cell line (Fig. 6a-d). When cells were cultivated on PLGA containing no ZnO-NPs, all parameters under consideration did not change and were at the level of the "control" group. About 4% of non-viable cells were observed; 1.3% of cells showed mitotic activity; the culture density was ~1200 cells/mm^2, ~30% of the polymer area was occupied by cells. It is noteworthy that the formation of a single monolayer was not observed. PLGA is often used to accelerate tissue regeneration and coating of nanomaterials in order to reduce the cytotoxic effect [37,38]. Functionalization of PLGA with ZnO-NPs led to an increase in the percentage of nonviable cells. When using the PLGA/ZnO-NPs composite with the maximum concentration of ZnO-NPs (0.1%), a decrease in the number of viable cells to ~92% and an increase in the cell-free surface compared to cultures growing on cultural plastic ("control") by ~5%. However, these changes are not critical for cell cultures. Thus, it was found that the surface of the synthesized composite material PLGA/ZnO-NP composite was suitable for adhesion, growth, and development of SH-SY5Y cell cultures and was not toxic to this cell line.

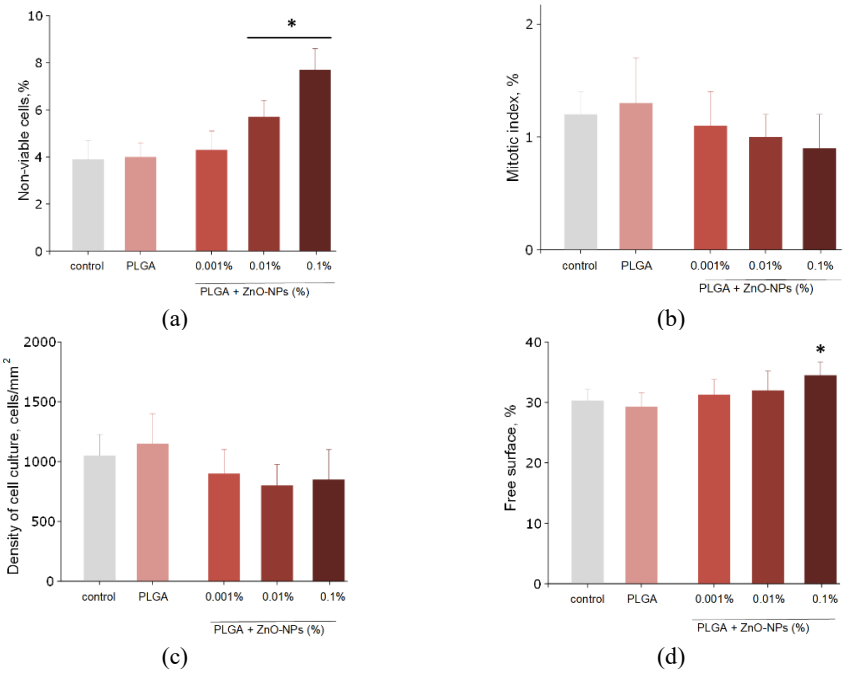

(a) (b) (c) (d)

Fig. 5. Effect of the PLGA/ZnO-NPs composite material on the main characteristics of the growth and development of human neuroblastoma cell line SH-SY5Y after 72 hours of in vitro cultivation. Viability of cell cultures (a); mitotic index of cells (b); cell culture density (c); colonization of the free surface by cells (d). * - statistically significant difference with the control group ($p<0.05$). Data are presented as mean with SEM.

4 Conclusions

A composite material based on PLGA functionalized with nanosized ZnO was obtained using a low-temperature method. It was shown that the resulting composite material is capable of generating ROS and, potentially, causing damage to DNA and proteins of bacterial cells. The composite with the addition of ZnO-NPs in PLGA, even at the minimum concentration (0.001%), significantly reduced the growth of *E. coli* bacteria. At the same time, the resulting composite was not toxic to SH-SY5Y cells. The PLGA/ZnO-NPs composite material is of great interest for biomedical use as well as for the food industry due to the controlled biodegradability of the material and its bioactive properties against bacterial cells.

Acknowledgements

This work was supported by a grant of the Ministry of Science and Higher Education of the Russian Federation (075-15-2022-315) for the organization and development of a World-class research center “Photonics”.

References

1. M. O. Paskhin, D. V. Yanykin, S. V. Gudkov, Horticulturae, **8**, 885 (2022).
2. J. R. Heath, Proc. of the Nat. Acad. of Sci., **112**, 14436-14443 (2015).
3. B. S. Sekhon, Nanotech., sci. & app., **3**, 1 (2010).
4. V. K. Truong, N. P. Truong, S. A. Rice, Antibact. Act. of Nanop., **11**, 1391 (2021).
5. A. Sirelkhatim, S. Mahmud, A. Seeni, N. H. M. Kaus, L. C. Ann, S. K. M. Bakhori, H. Hasan, D. Mohamad, Nano-micro lett., **7**, 219-242 (2015).
6. M. Alavi, A. Nokhodchi, Drug Discovery Today., **26**, 1953-1962 (2021).
7. T. S. Aldeen, H. E. A. Mohamed, M. Maaza, J. of Phys. & Chem. of Solids, **160**, 110313 (2022).
8. S. V. Gudkov, D. E. Burmistrov, D. A. Serov, M. B. Rebezov, A. A. Semenova, A. B. Lisitsyn, Front. in Phys., **9**, 641481 (2021).
9. B. L. da Silva, M. P. Abuçafy, E. B. Manaia, J. A. O. Junior, B. G. Chiari-Andréo, R. C. R. Pietro, L. A. Chiavacci, Int. J of nanomed., **14**, 9395 **(**2019).
10. A. Joe, S.-H. Park, K.-D. Shim, D.-J. Kim, K.-H. Jhee, H.-W. Lee, C.-H. Heo, H.-M. Kim, E.-S Jang, J. of Ind. and Eng. Chem., **45**, 430-439 (2017).
11. Y. Jo, E. Choi, N. Choi, C. Kim, Indust. & Eng. Chem. Res., **55**, 7801-7809 (2016).
12. A. Matei, I. Cernica, O. Cadar, C. Roman, V. Schiopu, Int. J. of Mat. Form., 767-770 (2008).
13. J. Li, R. Hong, M. Li, H. Li, Y. Zheng, J. Ding, Prog. in Org. Coat., **64**, 504-509 **(**2009).

14. C. V. Rocha, V. Gonçalves, M. C. da Silva, M. Bañobre-López, J. Gallo, Int. J. of Mol. Sci., **23**, 2034 (2022).
15. A. Parmar, G. Kaur, S. Kapil, V. Sharma, S. Sharma, App. Nanosci., **9**, 2001-2016 (2019).
16. M. S. Strozyk, D. J. de Aberasturi, J. V. Gregory, M. Brust, J. Lahann, L. M. Liz-Marzán, Adv. Funct. Mat., **27**, 1701626 (2017).
17. S. Xiong, S. George, H. Yu, R. Damoiseaux, B. France, K. W. Ng, J. S.-C. Loo, Archi. of toxicol., **87**, 1075-1086 (2013).
18. K. Huang, Z. Jinzhong, T. Zhu, Y. Morsi, A. Aldalbahi, M. El-Newehy, X. Yan, X. Mo, J. of Mat. Chem. B., **9**, 1452-1465 (2021).
19. C. Martins, F. Sousa, F. Araujo, B. Sarmento, Advanced healthcare materials, **7**, 1701035 (2018).
20. E. V. Barmina, I. A. Sukhov, G. Viau, G. A. Shafeev, Chem. Phys. Chem., **18**, 1069-1073 (2017).
21. M. A. Kaplan, K. V. Sergienko, A. A. Kolmakova, S. V. Konushkin, A. S. Baikin, A. G. Kolmakov, M. A. Sevostyanov, A. V. Kulikov, V. E. Ivanov, K. N. Belosludtsev, J. of Biomat. Sci., Pol. E., **31**, 1405-1420 (2020).
22. S. Gudkov, G. Lyakhov, V. Pustovoy, I. Shcherbakov, Phys. of Wave Phen., **27**, 141-144 (2019).
23. S. Gudkov, S. Garmash, I. Shtarkman, A. Chernikov, O. Karp, V. Bruskov, Biochem. & Biophys., 1 (2010).
24. S. V. Gudkov, E. L. Guryev, A. B. Gapeyev, M. G. Sharapov, N. F. Bunkin, A. V. Shkirin, T. S. Zabelina, A. P. Glinushkin, M. A. Sevost'yanov, K. N. Belosludtsev, Nanomed.: Nanotech., Bio. and Med., **15**, 37-46 (2019).
25. T. Okada, M. Kawakami, A.B. Hartanto, Y. Nakata, In Proc. of the Phot. Proc. in Microel. and Phot. II, 362-368 (2003).
26. M. C. Sportelli, M. Izzi, A. Volpe, M. Clemente, R. A. Picca, A. Ancona, P. M. Lugarà, G. Palazzo, N. Cioffi, Antibiotics, **7**, 67 (2018).
27. N. Babayevska, Ł. Przysiecka, I. Iatsunskyi, G. Nowaczyk, M. Jarek, E. Janiszewska, S. Jurga, Sci. Rep., **12**, 1-13 (2022).
28. J. A.-D. Olmo, L. Ruiz-Rubio, L. Pérez-Alvarez, V. Sáez-Martínez, J.L. Vilas-Vilela, Coat, **10**, 139 (2020).
29. M. Cloutier, D. Mantovani, F. Rosei, Tr. in biotech., **33**, 637-652 (2015).
30. L. Zuo, T. Zhou, B. Pannell, A. Ziegler, T.M Best, Act. Physiolog., **214**, 329-348 (2015).
31. X. Zhao, K. Drlica, Curr. Opin. in Microbiol., **21**, 1-6 (2014).
32. P. Fortini, B. Pascucci, E. Parlanti, M. D'errico, V. Simonelli, E. Dogliotti, Mut. Res./Fund. & Mol. Mech. of Mut., **531**, 127-139 (2003).
33. T. Yu, J. Slone, W. Liu, R. Barnes, P.L. Opresko, L. Wark, S. Mai, S. Horvath, T. Huang, Aging cell, e13669 (2022).
34. V. E. Ivanov, A. M. Usacheva, A. V. Chernikov, V. I. Bruskov, S. V. Gudkov, J. of Photochem. & Phot. B: Bio., **176**, 36-43 (2017).
35. S. V. Gudkov, D. E. Burmistrov, D. A. Serov, M. B. Rebezov, A. A. Semenova, A. B. Lisitsyn, Antibiotics, **10**, 884 (2021).
36. S. V. Gudkov, D. E. Burmistrov, V. V. Smirnova, A. A. Semenova, A. B. Lisitsyn, Nanomaterials, **10**, 884 (2022).

37. J. Qian, W. Xu, X. Yong, X. Jin, W. Zhang, Mat. Sci. & Eng., **36**, 95-101 (2014).
38. Z. Hajikarimi, S. Khoei, S. Khoee, S.R. Mahdavi, IEEE trans. on nanobiosci., **13**, 403-408 (2014).